Gene 936 (2025) 149093

Contents lists available at ScienceDirect

Gene

journal homepage: www.elsevier.com/locate/gene

Genetic and epigenetic factors affecting carotid intima-media thickness in monozygotic twins

Saho Mori [a], Yuya Arakawa [a,b], Mika Hasegawa [a], Shiho Kato [a], Hinako Hashimoto [a], Saki Yoshioka [a], Hiromichi Ueda [a], Osaka Twin Research Group [b], Mikio Watanabe [a,b,*]

[a] Department of Clinical Laboratory and Biomedical Sciences, Osaka University Graduate School of Medicine, Yamadaoka 1−7, Suita, Osaka, Japan
[b] Center for Twin Research, Osaka University Graduate School of Medicine, Yamadaoka 1−7, Suita, Osaka, Japan

ARTICLE INFO

Edited by: Nicola Lopizzo

Keywords:
Intima-media thickness
Subclinical atherosclerosis
Carotid ultrasonography
Single nucleotide polymorphisms
DNA methylation
RNA sequencing
Twin study

ABSTRACT

Background and aims: The intima-media thickness (IMT) of the carotid artery, an indicator of subclinical atherosclerosis, varies in close association with various factors such as diabetes and immune response. The extent of changes in IMT varies among individuals owing to both genetic and epigenetic factors. In this study, we aimed to identify single nucleotide polymorphisms (SNPs) and DNA methylation patterns that affect carotid IMT in monozygotic (MZ) twins.

Methods: We measured the maximum IMT (IMT-Cmax) and the mean IMT in the common carotid artery wall using ultrasonography in 107 pairs of MZ twins recruited from the Osaka University Twin Registry. The genotyping of SNPs and the measurement of methylation levels were performed using a beads array, and the expression of each gene was determined by RNA sequencing. Linear regression analysis was performed on each of the two groups: one group consisted of twins randomly selected from each pair, and the other group consisted of co-twins.

Results: We identified a CpG site (cg02432467) on *HS3ST6* as a significant epigenetic factor in both IMT-Cmax and mean IMT analyses. The methylation level at another site (cg07927379) was negatively correlated with *LINC01006* expression and IMT-Cmax. Furthermore, there were significant differences in *AP2A2* expression and mean IMT among individuals with each genotype of the rs10902263 polymorphism.

Conclusions: We identified genetic and epigenetic factors associated with carotid IMT that may be useful for individualized assessments.

1. Introduction

Atherosclerosis causes ischemic heart disease and stroke. Atherosclerosis is initiated by damage to vascular endothelial cells caused by risk factors such as hypertension, diabetes mellitus, and dyslipidemia (Gimbrone and García-Cardeña, 2016). Additionally, the lesion formation in atherosclerosis involves an immune response, including the infiltration of immune cells such as macrophages and T lymphocytes, and inflammatory responses induced by cytokines secreted by these cells (Hansson and Hermansson, 2011; Roy et al., 2022). One of the evaluation indices of subclinical atherosclerosis is the carotid artery intima-media thickness (IMT) measured by ultrasonography (Jilani et al., 2020). Carotid IMT is defined as the combined thickness of the intimal and medial layers of the carotid artery. Common carotid IMT is related to the future development of cardiovascular disease (Lorenz et al., 2006; Rosvall et al., 2005). The maximum and mean IMT, which represent the maximum area of thickening including plaque and the average value of IMT measured in a plaque-free area, respectively, are mainly used to evaluate subclinical atherosclerosis (Ling et al., 2023). Their combination may predict the onset of cardiovascular disease more accurately (Amato et al., 2017; Nambi et al., 2010). In a Vietnamese twin study, genetic influence on carotid IMT was reported to be approximately 60 %, while the remainder due to non-shared environmental influence (Zhao et al., 2008). Additionally, individuals with the AA genotype of

Abbreviations: IMT, Intima-media thickness; IMT-Cmax, maximum IMT; SNPs, single nucleotide polymorphisms; MZ, monozygotic; CpG, cytosine-phosphoguanine; SBP, systolic blood pressure; BMI, body mass index; BP, blood pressure.

* Corresponding author at: Department of Clinical Laboratory and Biomedical Sciences, Osaka University Graduate School of Medicine, Yamadaoka 1−7, Suita, Osaka 565−0871, Japan

E-mail address: nabe@sahs.med.osaka-u.ac.jp (M. Watanabe).

https://doi.org/10.1016/j.gene.2024.149093
Received 8 May 2024; Received in revised form 11 November 2024; Accepted 12 November 2024
Available online 14 November 2024

the rs780094 polymorphism in *GCKR* showed significantly reduced carotid IMT compared with individuals with the GG genotype (Murata-Mori et al., 2014). Furthermore, the hypermethylation of the methylation site on *ABCG1*, which plays a role in lipid metabolism, is significantly associated with an increased common carotid IMT (Qin et al., 2019). These results suggest that the genetic and epigenetic factors may affect to the increase in IMT.

The identification of genetic and epigenetic factors involved the subclinical atherosclerosis has the potential to establish predictive indicators for the onset of atherosclerosis. Therefore, in this study, we focused on single nucleotide polymorphisms (SNP) as a genetic factor and the DNA methylation of cytosine-phospho-guanine (CpG) sites as an epigenetic factor. We aimed to identify factors that contribute to an increase in IMT and are closely related to the pathogenesis of subclinical atherosclerosis. To conduct a stricter analysis considering the genetic background, we used monozygotic (MZ) twins as subjects because each pair had the same genetic factors.

2. Materials and methods

2.1. Subjects

Japanese MZ twins were recruited from the registry established by the Center for Twin Research, Osaka University Graduate School of Medicine (Honda et al., 2019). Participants with a self-reported history of stroke or myocardial infarction were excluded. Finally, we have analyzed 107 pairs (33 male and 74 female pairs) (Table 1). Written informed consent was obtained from all the twins, and this study protocol was approved by the Ethics Committee of Osaka University (Nos. 696 and 10209). The zygosity of the twin pair was confirmed by the perfect matching of 15 short tandem repeat loci using the PowerPlex 16 system (Promega, Madison, WI, USA). Medical and clinical examination, and carotid ultrasonography were also performed. The twins were examined on the same day.

2.2. Clinical parameters

Information regarding lifestyle and medication use was assessed using health-related questionnaires. Their weight, height, systolic blood pressure (SBP), and diastolic blood pressure were recorded. The body mass index (BMI) was calculated as weight in kilograms/ (height in meters)^2 (kg/m^2). Blood pressure (BP) was measured thrice with the UA-786 Blood Pressure Monitor (A&D Co. Ltd., Japan) in the sitting position. The average of the three BP measurements was used in the analysis.

Venous blood samples were collected at 9:00AM after a 12-h fast. Eight traits, namely HbA1c, fasting glucose, total cholesterol, triglycerides, high-density lipoprotein, low-density lipoprotein, uric acid, and creatinine were measured according to the methods of the IFCC Project (Ichihara, 2014).

2.3. Carotid ultrasonography

Ultrasonography was performed to evaluate carotid IMT and plaque formation using an ultrasound machine (Xario SSA-660A; Canon Medical Systems Inc, Japan) and a 7.5 MHz linear transducer (PLT-704SBT; Toshiba Medical Systems, Japan). We defined the distance from the lumen-intima interface to the media-adventitia interface as IMT. First, we observed IMT between the origin of the common carotid artery on the central side and a point 15 mm distal to the central side from the bifurcation of the internal and external carotid arteries on the longitudinal and transverse sections; the thickest IMT, including plaques, was determined as the maximal IMT (IMT-Cmax). Second, in the longitudinal view, we measured the following three points in the plaque-free region on the far wall: (i) maximal IMT, (ii) a point 10 mm distal to the maximal IMT, and (iii) a point 10 mm the proximal to the maximal IMT. The mean IMT was calculated as the average IMT at the three points (Irie et al., 2012). Ultrasound scans were performed by several examiners and images were saved in JPEG format. Image analysis was then performed by one analyst using ImageJ (National Institutes of Health, Bethesda, MD, USA), an image processing software. The IMT-Cmax and mean IMT were measured in both the left and right common carotid arteries, and the higher measurement values were used in the analysis. we did not consider the cardiac cycle and selected a time point at which IMT could be clearly observed because the effect of the cardiac cycle is only an error in the IMT measurement (Polak et al., 2012).

Table 1
Clinical characteristics of examined twins.

	All MZ twins	Female	Male	*p*-value
Number of samples	214 (107 pairs)	148 (74 pairs)	66 (33 pairs)	-
Age, years	53.1 ± 17.7 (20–88)	51.8 ± 16.5 (21–88)	56.2 ± 19.9 (20–85)	**0.045**
IMT-Cmax, mm	0.67 ± 0.43 (0.32–3.8)	0.65 ± 0.47 (0.32–3.8)	0.70 ± 0.29 (0.41–2.1)	**0.006**
Mean IMT, mm	0.53 ± 0.15 (0.26–0.98)	0.51 ± 0.15 (0.26–0.97)	0.59 ± 0.16 (0.33–0.98)	**0.001**
BMI, kg/m^2	21.7 ± 3.14 (14.1–32.9)	21.1 ± 2.63 (14.1–28.6)	22.8 ± 3.8 (15.5–32.9)	**0.003**
SBP, mmHg	122.1 ± 18.5 (88.0–179.0)	118.8 ± 17.3 (88.0–179.0)	129.6 ± 19.1 (88.0–175.0)	< **0.001**
DBP, mmHg	77.0 ± 11.3 (54.0–115.0)	75.5 ± 10.9 (54.0–115.0)	80.3 ± 11.6 (57.0–111.0)	**0.002**
HbA1c, %	5.4 ± 0.59 (4.2–9.0)	5.4 ± 0.60 (4.2–9.0)	5.5 ± 0.60 (4.6–7.1)	**0.031**
Fasting glucose, mg/dL	95.2 ± 14.1 (66.4–168.9)	93.3 ± 14.1 (66.4–168.9)	99.4 ± 13.2 (77.9–145.2)	< **0.001**
Total cholesterol, mg/dL	201.8 ± 35.0 (122.3–290.8)	204.3 ± 35.0 (122.3–290.8)	196.2 ± 34.7 (127.2–288.0)	0.175
Triglycerides, mg/dL	93.4 ± 58.0 (27.9–412.7)	85.2 ± 44.8 (27.9–299.2)	111.6 ± 77.4 (30.1–412.7)	**0.036**
HDL-c, mg/dL	63.9 ± 15.5 (32.4–111.2)	67.0 ± 15.5 (35.4–111.2)	56.8 ± 13.1 (32.4–89.6)	< **0.001**
LDL-c, mg/dL	118.6 ± 28.8 (59.6–216.7)	118.2 ± 28.3 (65.8–216.7)	119.4 ± 30.1 (59.6–215.9)	0.700
Uric acid, mg/dL	5.0 ± 1.2 (2.6–9.1)	4.6 ± 1.0 (2.6–7.2)	5.8 ± 1.1 (3.7–9.1)	< **0.001**
Creatinine, mg/dL	0.76 ± 0.16 (0.45–1.3)	0.69 ± 0.12 (0.45–1.3)	0.92 ± 0.11 (0.67–1.3)	< **0.001**
Smoking (%)	41 (19.2 %)	14 (9.5 %)	27 (40.9 %)	< **0.001**
Drinking (%)	126 (58.9 %)	76 (51.4 %)	50 (75.8 %)	< **0.001**
Exercise (%)	136 (63.6 %)	88 (59.5 %)	48 (72.7 %)	0.063
Hypertension medication (%)	29 (13.6 %)	16 (10.8 %)	13 (19.7 %)	0.079
Diabetes mellitus medication (%)	9 (4.2 %)	8 (5.4 %)	1 (1.5 %)	0.190
Hyperlipidemia medication (%)	20 (9.3 %)	15 (10.1 %)	5 (7.6 %)	0.552

DBP: Diastolic blood pressure.
[a]All values are given as n (%) or means ± standard deviations, and minimum to maximum.
[b]b. BMI: Body mass index. SBP: Systolic blood pressure.

2.4. Genotyping and imputation

SNP genotyping was performed using Illumina Infinium HumanOmni5-Quad v1-0 BeadChips (Illumina, San Diego, CA, USA) and Illumina Infinium HumanOmni v1-1 BeadChips (Illumina). Sample exclusion was performed following the criteria given below: (i) sample call rate < 0.98, (ii) closely related individuals identified by the identity-by-descent analysis, and (iii) East Asian outliers identified by the principal component analysis of the studied samples and the three major reference populations (Africans, Europeans, and East Asians) in the

International HapMap Project (International HapMap, C, The International HapMap Project, Nature, 2003). Variants were then subjected to the following standard quality-control criteria for exclusion (i) SNP call rate < 0.95, (ii) minor allele frequency < 1 %, and (iii) Hardy-Weinberg equilibrium *p*-value < 1.0e-07. Genotypes prephasing and imputation were performed using SHAPEIT and minimac and the 1000 Genomes Project Phase1 (version 3) East Asian reference haplotypes, respectively. For the X chromosome, prephasing and imputation was performed separately for females and males. A total of 107 samples and 39,692,293 variants were retained after edits.

2.5. DNA methylation data

DNA methylation levels were evaluated using Infinium HumanMethylation450 BeadChip Kit (Illumina) and the Infinium HumanMethylationEPIC BeadChip Kit (Illumina) according to the manufacturer's standard protocol, which interrogated over 450,000 highly informative CpG sites at a single-nucleotide resolution for each sample, which were shared by both arrays. The experiment was performed with 0.5 μg of high-quality genomic DNA. On the chip, there were two bead types for each CpG site per locus. The raw data were analyzed using the Genome Studio software (Illumina), and the fluorescence intensity ratios between the two bead types were calculated. A ratio of 0 indicated the non-methylation of the locus, and a ratio of 1 indicated complete methylation.

Finally, each methylation level was standardized by a regulation method using the proportions of granulocytes, monocytes, neutrophils, eosinophils, and basophils for linear model analysis (Jones et al., 2017).

2.6. RNA sequencing

Peripheral blood samples were stabilized and frozen in Tempus™ Blood RNA Tube (Applied Biosystems™) (Thermo Fisher Scientific, Inc, Waltham, MA, USA). RNA was extracted from the samples using Tempus Spin RNA Isolation Kit (Thermo Fisher Scientific) and ribosomal RNA and Globin mRNA were depleted using TruSeq Stranded Total RNA LT Sample Prep Kit (Illumina), according to the manufacturer's protocol (Martin and Wang, 2011). Gene expression was measured using Illumina NovaSeq 6000 (Illumina). We used Transcripts Per Kilobase Million (TPM) counts as normalization values for analysis. The expression of each gene was calculated using the following formula: $\log_2(\mathrm{TPM} + 1)$.

2.7. Adjusting IMT measurement value

The IMT values were adjusted for age, sex, and SBP using a linear regression model. The variables used for adjustment were selected by the multiple regression analysis of factors affecting IMT (Table 1). Finally, we normalized the residuals by applying an appropriate trait-specific transformation (Z-score) and used these values for further analyses.

2.8. Classification of MZ pairs

We classified MZ pairs into two groups: one consisted of randomly selected twins from all examined pairs (Twin1 group), and the other consisted of co-twins (Twin2 group). Since the Twin1 and Twin2 groups have the same basic characteristics, including sex, age, and genetic factors, these two groups were considered replicated subject groups. No significant differences were found between the two groups regarding IMT, SBP and BMI values (Supplementary Table 1).

2.9. Statistical analysis

We conducted linear regression analysis using R 4.0.1 and PLINK (ver 1.90b6.21). In the epigenome-wide association study (EWAS) and genome-wide association study (GWAS), *p*-values < 1.0E-07 and < 5.0E-08 were the thresholds for significance (before Bonferroni correction). The Wilcoxon rank-sum test or chi-square test was used to compare the characteristics of the samples. Multiple regression analysis was performed to minimize Akaike's Information Criterion using the JMP16 software (SAS Institute Inc., Cary, NC, USA).

3. Results

3.1. EWAS for carotid IMT

To investigate the DNA methylation levels of CpG sites affecting to carotid IMT, we performed EWAS in the Twin1 and Twin2 groups. The EWAS for IMT-Cmax revealed many significant CpG sites in each group; however, none of these CpG sites were common between the two groups (Supplementary Figure 1A). However, we detected 14 common CpG sites between the Twin1 and Twin2 groups among each suggestive CpG sites (Table 2A and Supplementary Figure 1A). In contrast, in the EWAS for the mean IMT, we could not find any CpG sites common between the Twin1 and Twin2 groups among the suggestive CpG sites (Supplementary Figure 1B). However, among the CpG sites from the lowest *p*-values to the 1000th CpG site, 21 CpG sites common to both groups were identified (Table 2B). Furthermore, we analyzed the correlation between the carotid IMT and the methylation level of each of the 21 CpG sites and found a significant positive correlation between the methylation level of the cg02432467 site, IMT-Cmax, and mean IMT (Fig. 1A and B).

To identify the methylation levels of CpG sites independently associated with IMT-Cmax and mean IMT, we performed multiple regression analysis using the methylation levels of 21 CpG sites common to the Twin1 and Twin2 groups and identified several CpG sites for each analysis (Table 3). Among them, the methylation level of the cg02016723 site was commonly associated with IMT-Cmax, whereas that of the cg26233408 site was commonly associated with mean IMT (Table 3).

Additionally, we focused on genes with common suggestive CpG sites using EWAS (Table 2) and analyzed the correlation between the methylation level of each CpG site and the gene expression level (Supplementary Table 2). The methylation level of the cg07927379 site on *LINC01006* was negatively correlated with gene expression and the adjusted IMT-Cmax (Fig. 1C and 1D). In contrast, there was a positive correlation between the methylation level of cg02016723 and *WFDC* expression (Supplementary Table 2).

3.2. GWAS for carotid IMT

To identify SNPs associated with carotid IMT, a GWAS was performed in the Twin1 and Twin2 groups (Supplementary Figure 2). No SNPs were significantly associated with the IMT-Cmax or mean IMT. However, we found seven suggestive SNPs in *SMYD3* for IMT-Cmax and one (rs10902263) in *AP2A2* for the mean IMT common to the Twin1 and Twin2 groups (*p*-value < 1.0E-04) with reproducibility (Supplementary Table 3).

Because the seven identified SNPs for the IMT-Cmax gene were in a linkage disequilibrium, we focused on rs1934578 as a representative and compared the expression of *SMYD3* and adjusted IMT-Cmax among the genotypes of this SNP. Additionally, *AP2A2* expression and adjusted mean IMT were compared between the genotypes of rs10902263. Tthe genotype of rs1934578 did not affect *SMYD3* expression, but the rs1934578 TC genotype was related to a significant decrease in adjusted IMT-Cmax (Fig. 2A). *AP2A2* expression was significantly downregulated in the rs10902263 TT genotype compared with that in the GG genotype (Fig. 2B). The adjusted mean IMT was decreased significantly in the rs10902263 TG and TT genotypes compared with that in the GG genotype (Fig. 2B).

Table 2
Common CpG sites in EWAS between Twin1 and Twin2 groups.

	CpGID	Chr	Mapinfo	Gene	Position	*p*-value (Twin1)	*p*-value (Twin2)
(A) IMT-Cmax							
1	cg17429686	1	2639790	*TTC34*	3′UTR	6.62E-05	2.35E-05
2	cg14380444	1	8517475	*RERE*	Body	2.22E-06	6.60E-05
3	cg15649333	1	157239890	—	—	5.46E-05	7.45E-05
4	cg11006267	5	139637839	—	—	6.76E-05	9.11E-05
5	cg19500607	5	148654756	*HTR4*	TSS1500	1.33E-05	1.17E-05
6	cg04939662	6	5084104	—	—	7.54E-05	7.25E-05
7	cg08453194	6	41936660	*CCND3*	Body	4.62E-05	6.42E-08
8	cg06867285	7	80013646	—	—	6.36E-06	2.49E-05
9	cg07927379	7	156640414	*LINC01006*	Body	1.76E-05	7.65E-06
10	cg02432467	16	1913431	*HS3ST6*	Body	2.73E-05	2.27E-05
11	cg09744036	17	81962654	—	—	9.39E-05	3.34E-05
12	cg07544187	19	19540426	*CILP2*	Body	8.24E-05	5.55E-06
13	cg12497914	20	2693639	*EBF4*	Body	2.84E-05	7.48E-05
14	cg02016723	20	45114870	*WFDC5*	Body	3.89E-05	4.85E-05
(B) Mean IMT							
1	cg17721530	1	26227956	—	—	8.41E-04	1.53E-04
2	cg27379715	2	880304	—	—	4.19E-04	1.20E-04
3	cg19015611	2	70899316	—	—	8.27E-04	4.12E-06
4	cg08023416	2	102187327	*IL1RL2*	5′UTR	7.15E-04	1.18E-04
5	cg07263322	2	221793032	—	—	2.56E-04	2.55E-05
6	cg04413180	2	235938413	*AGAP1*	Body	5.00E-04	1.20E-04
7	cg01008097	4	109346476	—	—	8.99E-04	1.78E-04
8	cg02279591	5	95653624	*RFESD;SPATA9*	Body;5′UTR	8.13E-04	1.23E-04
9	cg23939866	5	154802292	*LARP1*	Body	4.83E-04	2.19E-04
10	cg14736087	6	24724309	—	—	6.83E-04	7.07E-05
11	cg04092581	6	69863906	—	—	8.41E-04	1.49E-04
12	cg18036998	7	151203456	—	—	9.45E-04	1.97E-04
13	cg17494438	10	49392698	*DRGX*	TSS1500	0.00107	5.44E-05
14	cg10671668	12	4810064	*GALNT8*	1stExon	1.52E-04	3.80E-05
15	cg03865604	12	121280083	*CAMKK2*	5′UTR	0.00108	1.99E-04
16	cg01775802	14	72478753	—	—	5.13E-04	1.04E-04
17	cg02432467	16	1913431	*HS3ST6*	Body	1.13E-04	1.24E-04
18	cg04520396	17	1682018	*PRPF8*	Body	4.20E-04	1.37E-04
19	cg25952886	17	32993633	*SPACA3*	Body	3.68E-04	1.79E-04
20	cg26233408	17	80236871	*SLC26A11*	Body	0.00103	1.11E-04
21	cg19352808	19	6737743	—	—	6.22E-04	2.93E-05

4. Discussion

In this study, we identified genetic and epigenetic factors affecting to carotid IMT. Among the CpG sites that showed common association between the Twin1 and Twin2 groups and IMT-Cmax (Table 2A), the cg02016723 site was located on *WFDC5*, which encodes a protease inhibitor (Kalinina et al., 2021). Proteases, such as neutrophil elastase and thrombin, play roles in thrombus formation and are involved in atherosclerosis pathogenesis (Slack and Gordon, 2019). Neutrophil elastase is associated with cholesterol accumulation and may increase the risk of atherothrombotic events (Dollery et al., 2003), and thrombin exacerbates the inflammatory cascade in atherosclerosis by activating protease-activated receptors (Grandoch et al., 2016). Therefore, we hypothesized that *WFDC5* may play a role in preventing atherosclerosis progression by inhibiting these proteases. Moreover, a weak positive correlation of the methylation level in this CpG site with the expression of WFDC5 was shown (Supplementary Table 2). However, the methylation level at this site also exerted a positive effect on IMT-Cmax in both the Twin1 and Twin2 groups (Table 3). As WFDC5 plays a protective role against atherosclerosis, we hypothesized that the increased methylation level on WFDC5 may be induced by increased IMT to suppress the atherosclerosis progression.

The cg26233408 site identified by EWAS on the mean IMT was located on *SLC26A11,* which is involved in glucose transport as a sulfate transporter (Vincourt et al., 2003). This gene is also associated with fasting blood glucose levels according to a twin study (Wang et al., 2020) and is a susceptibility gene for cardiovascular disease in patients with hypertension and diabetes mellitus (Song et al., 2021). Therefore, methylation at cg26233408 may contribute to IMT as a subclinical atherosclerotic risk factors for hyperglycemia and hypertension.

The methylation level of cg02432467 was positively correlated with both IMT-Cmax and mean IMT (Fig. 1A and B). This CpG site, located on *HS3ST6*, encodes a sulfotransferase involved in heparan sulfate synthesis (Bork et al., 2021). Heparan sulfate exhibits an anticoagulant function with heparin-like antithrombin cofactor activity (Shimada et al., 1991) and inhibits atherogenesis by suppressing inflammation and smooth muscle cell proliferation (Tran-Lundmark et al., 2008). Therefore, an increase in the methylation level of the cg02432467 site probably suppresses sulfate transfer to heparan sulfate via *HS3ST6* and increases IMT.

Interestingly, a significant negative correlation was observed between the methylation level of the cg07927379 site and both *LINC01006* expression and adjusted IMT-Cmax (Fig. 1C and D). *LINC01006* expression in peripheral blood was significantly upregulated in patients with rheumatoid arthritis (Wen et al., 2020). *LINC01006* promotes the proliferation, migration, and invasion of tumor cells in various cancers (Ma et al., 2020; Song et al., 2021). This suggests that upregulated *LINC01006* expression due to the decrease in the methylation level of this CpG site augments the inflammatory response and leukocyte function; thereby increasing IMT.

According to the analysis of the genetic background, the seven SNPs on *SMYD3* affected IMT-Cmax (Supplementary Table 3A). *SMYD3* regulates *FOXP3* expression, a master transcription factor of regulatory T cells (Tregs) (McCaffrey et al., 2021), and *SMYD3* and *FOXP3* expressions are positively correlated (Nagata et al., 2015). Tregs suppress the immune responses of $CD4^+$ T cells and atherogenesis (Kasahara et al., 2022; Saigusa et al., 2020). In our study, adjusted IMT-Cmax increased significantly in individuals with the rs1934578 CC genotype (Fig. 2A). This suggests that in individuals with the rs1934578 CC genotype, *SMYD3* may suppress *FOXP3* expression more than in those with other

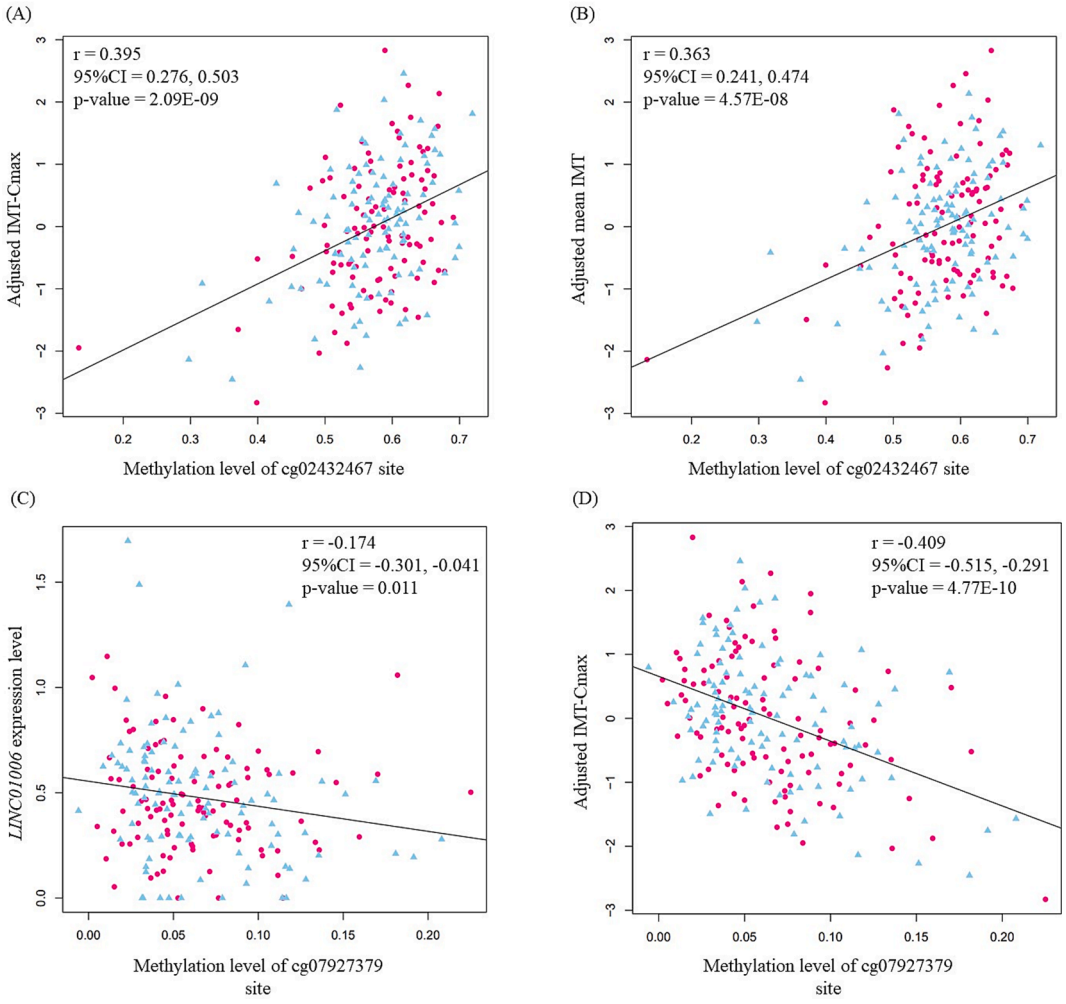

Fig. 1. Correlation between methylation levels and traits at cg02432467 and cg07927379 sites. Correlation between methylation levels in cg02432467 and (A) adjusted IMT-Cmax and (B) adjusted mean IMT. Correlation between the methylation levels of cg07927379 and (C) LINC01006 levels and (D) adjusted IMT-Cmax. The red circles and blue triangles represent Twin1 and Twin2 groups, respectively. The black line indicates regression.

Table 3
Best fit models of multiple regression analysis.

IMT-Cmax				Mean IMT		
CpGID	**coefficient**	***p*-value**		**CpGID**	**coefficient**	***p*-value**
Twin1 group						
Intercept	−10.2	< 0.0001		Intercept	13.3	0.0207
cg14380444	2.49	0.0024		cg07263322	−3.72	0.0444
cg09744036	5.88	0.0252		cg02432467	4.09	0.0016
cg02016723	**5.76**	**0.0174**		**cg26233408**	**−13.3**	**0.0380**
Twin2 group						
Intercept	−6.00	< 0.0001		Intercept	9.37	0.0460
				cg19015611	−0.62	0.3407
cg08453194	8.36	< 0.0001		cg08023416	2.07	0.0164
cg02016723	**4.14**	**0.0151**		cg14736087	4.65	0.0108
				cg26233408	**−15.7**	**0.0030**

[a]CpG sites selected by multiple regression analysis commonly between Twin1 and Twin2 groups were presented as bold.

genotypes, thereby increasing IMT by suppressing Tregs.

The rs10902263 polymorphism on *AP2A2* was associated with the mean IMT (Supplementary Table 4B). *AP2A2* is part of the AP2 adapter complex, a novel target of peroxisome proliferator-activated receptor alpha (PPARα) in adipose tissues, and PPARα activation upregulates *AP2A2* expression and promotes lipolysis (Montgomery et al., 2019). The T allele and TT genotype of rs7396366; located near *AP2A2,* were associated with an increased risk and severity of cardiovascular disease (Wang et al., 2018). These results suggested that genotypes associated with downregulated *AP2A2* expression contributed to the IMT increase by suppressing lipolysis. However, in this study, individuals with the TG and TT genotypes of rs10902263, which showed downregulated *AP2A2* expression, were associated with a significant decrease in mean IMT compared with individuals with the GG genotype (Fig. 2B). Since *AP2A2* has also been reported to play an important role in hepatic insulin signaling and glucose uptake (Montgomery et al., 2019), it is possible

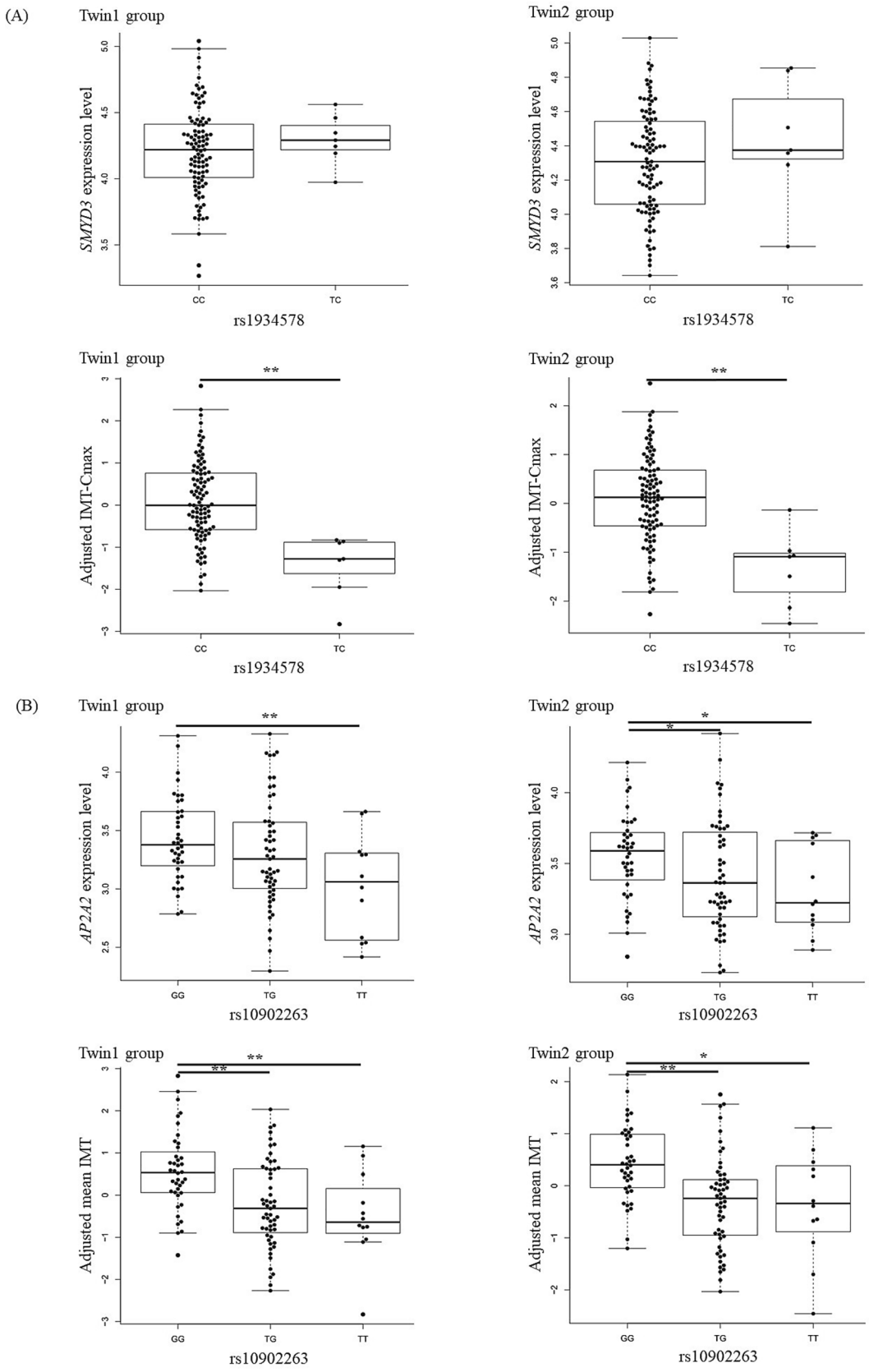

Fig. 2. Comparison of gene expression and carotid IMT by SNP genotypes. (A) SMYD3 expression and adjusted IMT-Cmax by rs1934578 genotypes were shown, respectively. (B) AP2A2 expression and adjusted mean IMT by rs10902263 genotypes were shown, respectively. *p-value < 0.05, **p-value < 0.01.

that AP2A2 regulates glucose metabolism and affects carotid IMT.

A limitation of this study is that we only have IMT data in common carotid artery, so we cannot examine blub IMT or internal carotid artery IMT, which will be more clinically important. However, genetic and environmental factors in IMT in common carotid artery will be relevant in other sites as well. In addition, the reliability of the results of this study may be limited due to the small sample size and the lack of another Japanese twin cohort to conduct replicate experiments. Furthermore, since the EWAS results in this study do not take into account causal relationships, it is unclear whether DNA methylation is a cause or a result of increased IMT.

4.1. Conclusions

SNPs and CpG methylation, which are closely associated with the pathogenesis of subclinical atherosclerosis, glucose metabolism, lipid metabolism, and leukocyte dynamics, have been identified as genetic and epigenetic factors affecting to common carotid IMT.

Financial support

This study was supported by JSPS KAKENHI (Grant No. A19H040480) and University Grants from the Japanese Ministry of Education, Culture, Sports, Science and Technology.

CRediT authorship contribution statement

Saho Mori: Writing – original draft, Visualization, Methodology, Formal analysis, Data curation. **Yuya Arakawa:** Writing – review & editing, Visualization, Data curation. **Mika Hasegawa:** Methodology, Formal analysis. **Shiho Kato:** Methodology, Formal analysis. **Hinako Hashimoto:** Methodology, Formal analysis. **Saki Yoshioka:** Methodology, Formal analysis. **Hiromichi Ueda:** Writing – review & editing, Methodology. **Osaka Twin Research Group:** Resources, Funding acquisition. **Mikio Watanabe:** Writing – review & editing, Supervision, Project administration, Funding acquisition.

Declaration of competing interest

The authors declare the following financial interests/personal relationships which may be considered as potential competing interests: [Mikio Watanabe reports financial support was provided by Japan Society for the Promotion of Science. Osaka Twin Research Group reports financial support was provided by Government of Japan Ministry of Education Culture Sports Science and Technology. Osaka Twin Research Group reports equipment, drugs, or supplies was provided by Beckman Coulter Inc. If there are other authors, they declare that they have no known competing financial interests or personal relationships that could have appeared to influence the work reported in this paper].

Acknowledgment

The authors extend their appreciation to the Specially Appointed Researcher Kanako Akada (Center for Twin Research at Osaka University Graduate School of Medicine). The authors also grateful to Beckman Coulter, Inc. (Tokyo, Japan) for their collaborative work.

Appendix A. Supplementary data

Supplementary data to this article can be found online at https://doi.org/10.1016/j.gene.2024.149093.

Data availability

The authors do not have permission to share data.

References

Amato, M., Veglia, F., de Faire, U., et al., 2017. Carotid plaque-thickness and common carotid IMT show additive value in cardiovascular risk prediction and reclassification. Atherosclerosis 263, 412–419.
Bork, K., Wulff, K., Möhl, B.S., et al., 2021. Novel hereditary angioedema linked with a heparan sulfate 3-O-sulfotransferase 6 gene mutation. J. Allergy Clin. Immunol. 148, 1041–1048.
Dollery, C.M., Owen, C.A., Sukhova, G.K., et al., 2003. Neutrophil elastase in human atherosclerotic plaques: production by macrophages. Circulation 107, 2829–2836.
Gimbrone Jr., M.A., García-Cardeña, G., 2016. Endothelial cell dysfunction and the pathobiology of atherosclerosis. Circ. Res. 118, 620–636.
Grandoch, M., Kohlmorgen, C., Melchior-Becker, A., et al., 2016. Loss of biglycan enhances thrombin generation in apolipoprotein E-deficient mice: implications for inflammation and atherosclerosis. Arterioscler. Thromb. Vasc. Biol. 36, e41–e50.
Hansson, G.K., Hermansson, A., 2011. The immune system in atherosclerosis. Nat. Immunol. 12, 204–212.
Honda, C., Watanabe, M., Tomizawa, R., et al., 2019. Update on osaka university twin registry: an overview of multidisciplinary research resources and biobank at osaka university center for twin research. Twin Res. Hum. Genet. 22, 597–601.
Ichihara, K., 2014. Statistical considerations for harmonization of the global multicenter study on reference values. Clin. Chim. Acta 432, 108–118.
International HapMap, C, The International HapMap Project, Nature, 2003;426:789-796.
Irie, Y., Katakami, N., Kaneto, H., et al., 2012. Maximum carotid intima-media thickness improves the prediction ability of coronary artery stenosis in type 2 diabetic patients without history of coronary artery disease. Atherosclerosis 221, 438–444.
Jilani, M.H., Simon-Friedt, B., Yahya, T., et al., 2020. Associations between particulate matter air pollution, presence and progression of subclinical coronary and carotid atherosclerosis: a systematic review. Atherosclerosis 306, 22–32.
Jones, M.J., Islam, S.A., Edgar, R.D., et al., 2017. Adjusting for cell type composition in DNA methylation data using a regression-based approach. Methods Mol. Biol. 1589, 99–106.
Kalinina, P., Vorstandlechner, V., Buchberger, M., et al., 2021. The whey acidic protein WFDC12 is specifically expressed in terminally differentiated keratinocytes and regulates epidermal serine protease activity. J, Invest. Dermatol. 141, 1198–1206.
Kasahara, K., Sasaki, N., Amin, H.Z., et al., 2022. Depletion of Foxp3(+) regulatory T cells augments CD4(+) T cell immune responses in atherosclerosis-prone hypercholesterolemic mice. Heliyon 8, e09981.
Ling, Y., Wan, Y., Barinas-Mitchell, E., et al., 2023. Varying definitions of carotid intima-media thickness and future cardiovascular disease: a systematic review and meta-analysis. J. Am. Heart Assoc. 12, e031217.
Lorenz, M.W., von Kegler, S., Steinmetz, H., et al., 2006. Carotid intima-media thickening indicates a higher vascular risk across a wide age range: prospective data from the Carotid Atherosclerosis Progression Study (CAPS). Stroke 37, 87–92.
Ma, E., Wang, Q., Li, J., et al., 2020. LINC01006 facilitates cell proliferation, migration and invasion in prostate cancer through targeting miR-34a-5p to up-regulate DAAM1. Cancer Cell Int. 20, 515.
Martin, J.A., Wang, Z., 2011. Next-generation transcriptome assembly. Nat. Rev. Genet. 12, 671–682.
McCaffrey, T.A., Toma, I., Yang, Z., et al., 2021. RNA sequencing of blood in coronary artery disease: involvement of regulatory T cell imbalance. BMC Med. Genomics 14, 216.
Montgomery, M.K., Bayliss, J., Keenan, S., et al., 2019. The role of Ap2a2 in PPARα-mediated regulation of lipolysis in adipose tissue. FASEB J. 33, 13267–13279.
Murata-Mori, F., Hayashida, N., Ando, T., et al., 2014. Association of the GCKR rs780094 polymorphism with metabolic traits including carotid intima-media thickness in Japanese community-dwelling men, but not in women. Clin. Chem. Lab. Med. 52, 289–295.
Nagata, D.E., Ting, H.A., Cavassani, K.A., et al., 2015. Epigenetic control of Foxp3 by SMYD3 H3K4 histone methyltransferase controls iTreg development and regulates pathogenic T-cell responses during pulmonary viral infection. Mucosal Immunol. 8, 1131–1143.
Nambi, V., Chambless, L., Folsom, A.R., et al., 2010. Carotid intima-media thickness and presence or absence of plaque improves prediction of coronary heart disease risk: the ARIC (Atherosclerosis Risk In Communities) study. J. Am. Coll. Cardiol. 55, 1600–1607.
Polak, J.F., Johnson, C., Harrington, A., et al., 2012. Changes in carotid intima-media thickness during the cardiac cycle: the multi-ethnic study of atherosclerosis. J. Am. Heart Assoc. 1, e001420.
Qin, X., Li, J., Wu, T., et al., 2019. Overall and sex-specific associations between methylation of the ABCG1 and APOE genes and ischemic stroke or other atherosclerosis-related traits in a sibling study of Chinese population. Clin. Epigenetics 11, 189.
Rosvall, M., Janzon, L., Berglund, G., et al., 2005. Incident coronary events and case fatality in relation to common carotid intima-media thickness. J. Intern. Med. 257, 430–437.
Roy, P., Orecchioni, M., Ley, K., 2022. How the immune system shapes atherosclerosis: roles of innate and adaptive immunity. Nat. Rev. Immunol. 22, 251–265.
Saigusa, R., Winkels, H., Ley, K., 2020. T cell subsets and functions in atherosclerosis. Nat. Rev. Cardiol. 17, 387–401.
Shimada, K., Kobayashi, M., Kimura, S., et al., 1991. Anticoagulant heparin-like glycosaminoglycans on endothelial cell surface. Jpn. Circ. J. 55, 1016–1021.
Slack, M.A., Gordon, S.M., 2019. Protease activity in vascular disease. Arterioscler. Thromb. Vasc. Biol. 39, e210–e218.

Song, Y., Choi, J.E., Kwon, Y.J., et al., 2021. Identification of susceptibility loci for cardiovascular disease in adults with hypertension, diabetes, and dyslipidemia. J. Transl. Med. 19, 85.
Song, Y., Wang, S., Cheng, X., 2021. LINC01006 regulates the proliferation, migration and invasion of hepatocellular carcinoma cells through regulating miR-433-3p/CBX3 axis. Ann. Hepatol. 25, 100343.
Tran-Lundmark, K., Tran, P.K., Paulsson-Berne, G., et al., 2008. Heparan sulfate in perlecan promotes mouse atherosclerosis: roles in lipid permeability, lipid retention, and smooth muscle cell proliferation. Circ. Res. 103, 43–52.
Vincourt, J.B., Jullien, D., Amalric, F., et al., 2003. Molecular and functional characterization of SLC26A11, a sodium-independent sulfate transporter from high endothelial venules. FASEB J. 17, 890–892.
Wang, S., Ma, Z., Zhang, Y., et al., 2018. A genetic variant near adaptor-related protein complex 2 alpha 2 subunit gene is associated with coronary artery disease in a Chinese population. BMC Cardiovasc. Disord. 18, 161.
Wang, W., Zhang, C., Liu, H., et al., 2020. Heritability and genome-wide association analyses of fasting plasma glucose in Chinese adult twins. BMC Genomics 21, 491.
Wen, J., Liu, J., Jiang, H., et al., 2020. lncRNA expression profiles related to apoptosis and autophagy in peripheral blood mononuclear cells of patients with rheumatoid arthritis. FEBS Open Bio 10, 1642–1654.
Zhao, J., Cheema, F.A., Bremner, J.D., et al., 2008. Heritability of carotid intima-media thickness: a twin study. Atherosclerosis 197, 814–820.